



Late Pleistocene glacial forest of Humaitá—Western Amazonia



M.C.L. Cohen^{a,b,*}, D.F. Rossetti^c, L.C.R. Pessenda^d, Y.S. Friaes^a, P.E. Oliveira^e

^a Post-Graduate Program of Geology and Geochemistry, Laboratory of Coastal Dynamics, Federal University of Pará, Avenida Perimentral 2651, Terra Firme, CEP: 66077-530, Belém, PA, Brazil

^b Faculty of Oceanography, Federal University of Pará, Rua Augusto Corrêa 1, Guama, CEP: 66075-110, Belém, PA, Brazil

^c National Space Research Institute (INPE), Rua dos Astronautas 1758-CP 515, CEP: 12245-970, São José dos Campos, SP, Brazil

^d Center for Nuclear Energy in Agriculture (CENA), University of São Paulo, 13400-000 Piracicaba, São Paulo, Brazil

^e São Francisco University, Av. São Francisco de Assis, 218, Jd. São José, Bragança Paulista, SP, Brazil

ARTICLE INFO

Article history:

Received 18 June 2013

Received in revised form 12 December 2013

Accepted 16 December 2013

Available online 23 December 2013

Keywords:

Alnus

Brazilian Amazonia

C isotope

Last Glacial Maximum

Palynology

Sedimentary facies

ABSTRACT

Glacial-aged vegetation dynamics of the Humaitá—Western Brazilian Amazonia were studied by pollen, sedimentary facies, ¹⁴C dating, $\delta^{13}\text{C}_{\text{org}}$ and $\text{C}/\text{N}_{\text{molar}}$. Two sediment cores were taken to a depth of 10 and 8 m from areas covered by grassland and dense/open forest, respectively. The deposits represent a succession of sediment accumulation in active channel (>42,600 cal yr B.P.), abandoned channel/floodplain (>42,600 to ~39,000 cal yr B.P.), and oxbow lake sedimentary environments (~39,000 cal yr B.P. to modern). The predominance of mud sediments, depletion of $\delta^{13}\text{C}_{\text{org}}$ and decrease in $\text{C}/\text{N}_{\text{molar}}$ values identify the lake establishment. In these settings, low energy subaqueous conditions were developed, locally favoring preservation of a pollen assemblage representing herbaceous vegetation, some modern taxa from Amazonia and cold-adapted plants from the Andes represented by *Alnus* (2–11%), *Hedyosmum* (2–17%), *Weinmannia* (0–18%), *Podocarpus* (0–4%), *Ilex* (0–4%) and *Drymids* (0–1%), at least between >42,600 and <35,200 cal yr B.P. The herbs and modern taxa from Amazonia persisted through the Holocene, while the cold pollen assemblage became absent. The co-occurrence of *Alnus* with other cold adapted plants from the Andes during the late Pleistocene indicates that *Alnus* probably penetrated the Western Amazonia lowland or was growing closer to the study site due to cooler temperatures during glacial times. The present study presents the first report of a glacial age forest containing *Alnus* in areas of the Brazilian Amazonian lowlands. In addition to its palaeogeographical importance, this work demonstrates the effectiveness of using a combination of proxies for reconstructing sedimentary environments associated with vegetation.

© 2013 Elsevier B.V. All rights reserved.

1. Introduction

The nature of the vegetation and climate within the Amazon basin during the Last Glacial Maximum (LGM) remains a subject of scientific debate. With regard to the humidity (e.g. Irion, 1982; Räsänen et al., 1987; Salo, 1987; Colinvaux et al., 2000), pollen studies estimate a range from invariant rainfall (Colinvaux, 1998) to a reduction of about 20–55% (Bush, 1994; van der Hammen and Absy, 1994; van der Hammen and Hooghiemstra, 2000). A biogeochemical record from Lagoa da Pata, Rio Negro basin, revealed three hydrological and climatic regimes. The first phase, between 50,000 and 26,300 cal yr BP, was characterized by a relatively wet climate. The second phase, between 26,300 and 15,300 cal yr BP, was characterized by a dry phase, and the third phase, from approximately 15,300 to 10,000 cal yr BP, was characterized by a wetter climate (Cordeiro et al., 2011). Due to this dry phase, the Amazon humid forest area probably shrank to 54% of their present-day extent during the LGM

(Anhuf et al. (2006)). However, speleothem oxygen isotope indicates that ecosystems in western Amazonia have not experienced prolonged drying over the past 94,000 years (Mosblech et al., 2012), and during the last glacial period, a modest increase in precipitation occurred in western Amazonia, whereas a significant drying occurred in eastern Amazonia (Cheng et al., 2013).

Unlike the paleoprecipitation records, there is greater agreement of cooler surface conditions during the LGM. Andean ice cores contain isotopic evidence that tropical late Pleistocene temperatures may have been depressed as much as 8–12 °C at high elevations (Thompson et al., 1998). Pollen records from Bolivia, Ecuador, Peru and Brazil provide evidence for cooling in glacial times (Liu and Colinvaux, 1985; Bush et al., 1990; Bush et al., 1992; De Oliveira, 1992; Ledru, 1993; Colinvaux et al., 1996a; Mourguiart and Ledru, 2003; Bush et al., 2004; Pessenda et al., 2009; Urrego et al., 2010). Also, downslope movement of montane elements such as *Podocarpus*, *Drymids*, *Hedyosmum* and *Alnus* occurred in mid-elevations in Amazonian areas during the LGM (Liu and Colinvaux, 1985; Bush et al., 1990; Colinvaux et al., 1997; Bush et al., 2004; Urrego et al., 2010).

Pollen in a sediment core sampled from Lake Consuelo (1360 m above sea-level, asl) adjacent to the Bolivian border in southeastern Peru indicates that the forest surrounding the lake was dominated

* Corresponding author at: Post-Graduate Program of Geology and Geochemistry, Laboratory of Coastal Dynamics, Federal University of Pará, Avenida Perimentral 2651, Terra Firme, CEP: 66077-530, Belém, PA, Brazil. Tel./fax: +55 91 3274 3069.

E-mail address: mcohen@ufpa.br (M.C.L. Cohen).

between 43.5 and 22 kcal yr B.P. by a mixture of upper montane and lowland elements. Upper montane taxa include *Alnus*, *Vallea*, *Podocarpus*, *Myrsine* and *Symplocos*, which are virtually absent from the modern pollen assemblage (Urrego et al., 2005). Palaeoecological studies in north-eastern Bolivia (600 to 900 m asl) near the southern margin of Amazonia identify the presence of pollen of *Podocarpus*, *Alnus* and *Ilex* between 50 kcal yr B.P. and the LGM (Burbridge et al., 2004). A palaeoclimate record from a shallow lake situated along the Paraguay River indicates that between ~45.0 and 19.5 kyr B.P. the climate was colder (4 °C lower compared to modern) and drier than present (Whitney et al., 2011). This set of records contributes to expanding the paleobotanical evidence (e.g., Behling, 1996; Behling et al., 1999; Colinvaux et al., 2000; Ledru et al., 2001) for cooler temperatures (5 °C below present) (Stute et al., 1995; Burbridge et al., 2004).

The LGM pollen cores for lowland Amazonia indicate also a cooling (Behling, 1996; Colinvaux et al., 1996b; Haberle and Maslin, 1999; Mayle et al., 2000; Ledru et al., 2001; Bush et al., 2004), and the few non-plant-based estimates of lowland temperature change suggest ~6 °C decrease from present from isotopic and elemental analyses of Caribbean corals (Guilderson et al., 1994) and Brazilian groundwater noble gases (Stute et al., 1995).

According to Bush (2002), the lowland forest in Amazonia contained significant populations of plants typical of modern montane areas during the LGM. This finding suggests that during early Holocene global warming, plants intolerant to the warmer climate became extinct in the lowland forest (Colinvaux et al., 2000).

As a contribution towards further evaluation of the geographic expression of a cooler climate during the late Pleistocene and a warmer climate during the Holocene, we studied two sediment cores that accumulated during these periods on the left margin of the Madeira River, the largest tributary of the Amazon River (Fig. 1a). Based on multiple proxies, including sedimentary facies, pollen, $\delta^{13}\text{C}_{\text{org}}$, C/N_{molar} ratio, and AMS radiocarbon dating, this paper provides insight into the extent of cooler tropical temperature effects on lowlands (elevation of ~100 m) of the Western Amazon forest.

2. Study area

The study area is located between the city of Porto Velho, north of the State of Rondonia, and the town of Humaitá, south of the State of Amazonas in the Western Brazilian Amazonia (Fig. 1). It is characterized by tropical climate with a short dry season (Am in Köppen's classification), with mean annual temperature between 24 °C and 26 °C, and mean annual precipitation between 2250 and 2750 mm. The relative humidity in the region is 85%. Rainy periods begin in October, with precipitation peaks in January to February, while dry periods are between June and August (Brasil, 1978). The principal vegetation cover consists mostly of arboreal vegetation including dense and open forest and dense woodland savanna that are intermingled often in sharp contact with large patches of pioneer formations and natural grassland/shrubland savanna vegetation (Fig. 1a) (Brasil, 1978). These vegetation units are not subject to periodic flooding of fluvial waters. These areas of natural savanna vegetation around Humaitá cover 615 km² (Vidotto et al., 2007). In the study area, a large patch of open vegetation (mostly pioneer vegetation/grassland savanna) is present, which averages nearly 20 km in length and up to 10 km in width (Fig. 1a). The arboreal vegetation is mainly represented by Euphorbiaceae, Bignoniaceae, Fabaceae, Moraceae, Anacardiaceae, Malpighiaceae, Malvaceae, Sapotaceae, Rubiaceae and Apocynaceae, whereas herbs are mainly represented by Poaceae, Cyperaceae and Asteraceae. Near the sampling sites, 138 species and genera distributed among 37 families of arboreal and herbaceous vegetation were identified (Vidotto et al., 2007) (Table 1).

The region has a small elevation range (~100 m elevation, Fig. 1b). The Quaternary sediments (Pessenda et al., 2001; Latrubesse, 2002) occur mainly along the fluvial terraces and above the modern floodplain area with altitudinal variations ranging from 45 to 100 m. The region contains a paleomorphology recording a large riverine meander belt (Fig. 1a). This landscape consists of a semi-circular shape displaying a set of concentric lines, which is in sharp contact with surrounding areas. The geological setting of the study area is within the southwestern and southeastern part of the Solimões Basin, which is a foreland basin of

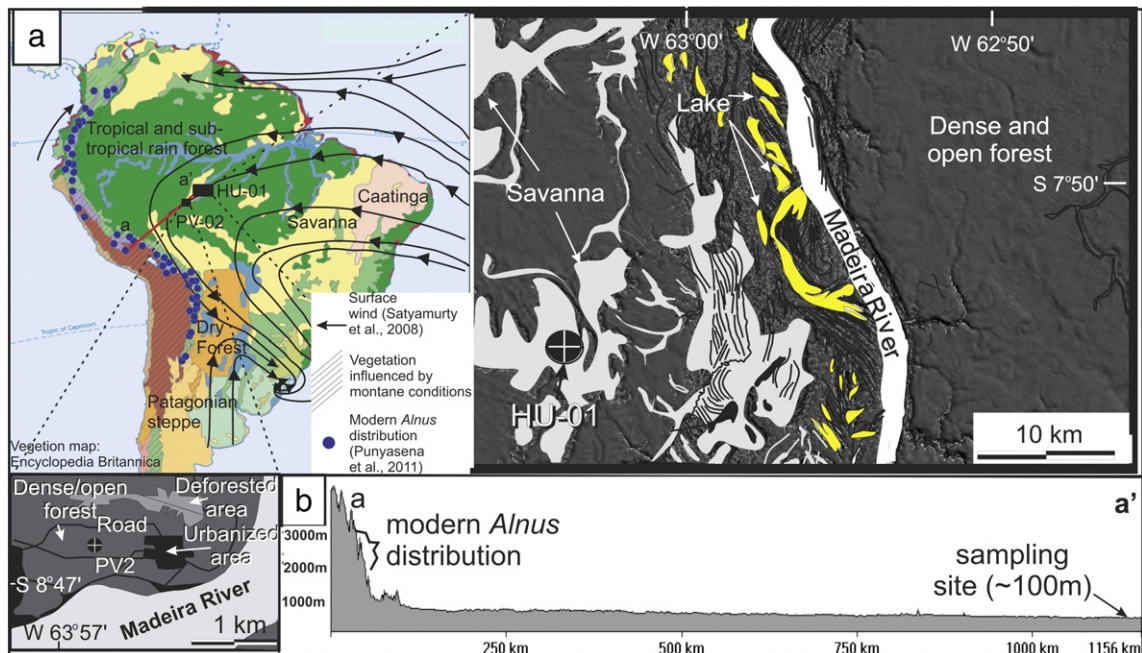


Fig. 1. a) Sediment core location, main geomorphologic features, surface wind directions, modern *Alnus* distribution, and location of vegetation units; b) topographic profile from Andes to study site.

Table 1

Taxa identified near the sampling sites (Vidotto et al., 2007). During the sampling of arboreal and herbaceous vegetation was used the methods of Quadrant Point (Cottam and Curtis, 1956) and Point Contact (Whitman and Siggeirsson, 1954), respectively.

Family and species	Biological form	Veg. units
Anacardiaceae		
<i>Tapirira guianensis</i> Aubl.	Arboreal	Forest
Annonaceae		
<i>Annona</i> sp1	Arboreal	Forest
<i>Annona</i> sp2	Arboreal	Forest
<i>Annona</i> sp3	Arboreal	Forest
<i>Annona</i> sp4	Arboreal	Forest
<i>Annona</i> sp5	Arboreal	Forest
<i>Annona</i> sp6	Arboreal	Forest
<i>Annona</i> sp7	Arboreal	Forest
<i>Guatteria</i> sp	Arboreal	Forest
<i>Xylopia aromatica</i>	Arboreal	Forest
Apocynaceae		
<i>Couma guianensis</i> Aubl.	Arboreal	Forest
<i>Geissospermum</i> aff. <i>urceolatum</i>	Arboreal	Forest
<i>Himatanthus sucuuba</i>	Arboreal	Forest
Araceae		
<i>Philodendron</i> sp	Epiphyte	Forest
Araliaceae		
<i>Schefflera morototoni</i>	Arboreal	Forest
Arecaceae		
<i>Allagoptera caudescens</i>		
<i>Astrocaryum acaule</i>	Arboreal	Forest
<i>Euterpe precatoria</i>	Shrub	Savanna
<i>Geonoma multiflora</i>	Shrub	Savanna
<i>Lepidocaryum tenue</i>		
<i>Mauritia flexuosa</i>	Arboreal	Forest
<i>Mauritiella armata</i>	Arboreal	Forest
<i>Oenocarpus bacaba</i>	Arboreal	Forest
<i>Oenocarpus bataua</i>	Arboreal	Forest
<i>Oenocarpus minor</i>	Arboreal	Forest
<i>Orbignya speciosa</i>	Arboreal	Forest
<i>Socratea exorrhiza</i>	Arboreal	Forest
Asteraceae		
<i>Eupatorium</i> sp	Herb	Savanna
<i>Vernonia herbacea</i>	Arboreal	Forest
Bignoniaceae		
<i>Jacaranda</i> sp 1	Arboreal	Forest
<i>Jacaranda</i> sp 2	Arboreal	Forest
Bromeliaceae		
<i>Ananas ananassoides</i>	Herb	Savanna
Burseraceae		
<i>Bursera</i> sp	Arboreal	Forest
<i>Hemicrepidospermum</i> sp	Arboreal	Forest
<i>Protium paniculatum</i>	Arboreal	Forest
<i>Protium</i> sp1	Arboreal	Forest
<i>Protium</i> sp2	Arboreal	Forest
Celastraceae		
<i>Goupia glabra</i>	Arboreal	Forest
Chrysobalanaceae		
<i>Couepia</i> sp	Arboreal	Forest
<i>Licania</i> sp1	Arboreal	Forest
Clusiaceae		
<i>Caraipa savannarum</i>	Arboreal	Forest
<i>Vismia cayennensis</i>	Arboreal	Forest
<i>Vismia guianensis</i>	Arboreal	Forest
<i>Vismia latifolia</i>	Arboreal	Forest
<i>Vismia</i> sp	Arboreal	Forest
Cyperaceae		
<i>Bulbostylis</i> sp	Herb	Savanna
<i>Cyperus</i> sp	Herb	Savanna
<i>Fimbristylis</i> sp	Herb	Savanna
<i>Kyllinga</i> sp	Herb	Savanna
<i>Rhynchospora</i> sp	Herb	Savanna
<i>Scleria</i> aff. <i>reflexa</i>	Herb	Savanna
Dilleniaceae		
<i>Curatella americana</i> L.	Arboreal	Forest
<i>Davilla rugosa</i> Poir	Liana	Forest
Euphorbiaceae		
<i>Hevea brasiliensis</i>	Arboreal	Forest
<i>Jatropha phyllacantha</i>	Arboreal	Forest
<i>Mabea caudate</i>	Arboreal	Forest
<i>Mabea subsessilis</i>	Arboreal	Forest

Table 1 (continued)

Family and species	Biological form	Veg. units
Fabaceae		
<i>Andira</i> sp	Arboreal	Forest
<i>Bauhinia guianensis</i> .	Arboreal	Forest
<i>Bauhinia</i> sp	Arboreal	Forest
<i>Dioclea</i> cf. <i>huberi</i> Ducke	Liana	Forest
<i>Dipteryx odorata</i> (Aubl.)	Arboreal	Forest
<i>Hymenaea</i> sp	Arboreal	Forest
<i>Inga</i> sp	Arboreal	Forest
<i>Mimosa</i> sp	Arboreal	Forest
<i>Ormosia</i> sp	Arboreal	Forest
<i>Sclerolobium paniculatum</i>	Arboreal	Forest
<i>Tachigali myrmecophilla</i>	Arboreal	Forest
Flacourtiaceae		
<i>Casearia grandiflora</i> Cambess.	Arboreal	Forest
<i>Casearia</i> sp	Arboreal	Forest
Heliconiaceae		
<i>Heliconia psittacorum</i>	Herb	Savanna
Lauraceae		
<i>Aniba</i> sp1	Arboreal	Forest
<i>Aniba</i> sp2	Arboreal	Forest
<i>Nectandra cuspidata</i>	Arboreal	Forest
<i>Nectandra lanceolata</i>	Arboreal	Forest
<i>Ocotea</i> sp1	Arboreal	Forest
<i>Eschweilera</i> sp	Arboreal	Forest
Linaceae		
<i>Ochthocosmus</i> cf. <i>barrae</i>	Arboreal	Forest
Lythraceae		
<i>Cuphea</i> sp	Herb	Savanna
<i>Physocalymma scaberrimum</i>	Arboreal	Forest
Malpighiaceae		
<i>Banisteriopsis</i> sp	Arboreal	Forest
<i>Byrsonima</i> sp1	Arboreal	Forest
<i>Byrsonima</i> sp2	Arboreal	Forest
<i>Byrsonima</i> cf. <i>verbascifolia</i>	Arboreal	Forest
Malvaceae		
<i>Hibiscus furcellatus</i>	Arboreal	Forest
Marantaceae		
<i>Monotagma</i> sp	Herb	Savanna
<i>Bellucia grossularioides</i>	Arboreal	Forest
<i>Miconia tiliifolia</i> Naudin	Arboreal	Forest
<i>Miconia</i> sp	Arboreal	Forest
<i>Miconia</i> sp3	Arboreal	Forest
Marantaceae		
<i>Tibouchina aspera</i>	Shrub	Savanna
<i>Tibouchina</i> sp	Arboreal	Forest
Monimiaceae		
<i>Siparuna guianensis</i>	Shrub	Savanna
<i>Siparuna</i> sp	Arboreal	Forest
Moraceae		
<i>Naucleopsis caloneura</i>	Arboreal	Savanna
Myristicaceae		
<i>Iryanthera</i> sp	Arboreal	Forest
<i>Virola sebifera</i>	Arboreal	Forest
<i>Virola surinamensis</i>	Arboreal	Forest
<i>Virola</i> sp	Arboreal	Forest
<i>Virola</i> sp2	Arboreal	Forest
Myrtaceae		
<i>Eugenia</i> sp1	Arboreal	Forest
<i>Eugenia</i> sp2	Arboreal	Forest
<i>Myrcia</i> sp	Arboreal	Forest
Piperaceae		
<i>Piper</i> sp 1	Shrub	Savanna
<i>Piper</i> sp 2	Shrub	Savanna
Poaceae		
<i>Andropogon bicornis</i> L.	Herb	Savanna
<i>Andropogon lanatus</i> R. Br.	Herb	Savanna
<i>Andropogon leucostachyus</i>	Herb	Savanna
<i>Aristida capillacea</i>	Herb	Savanna
<i>Axonopus aureus</i>	Herb	Savanna
<i>Lasiacis</i> cf. <i>ligulata</i>	Herb	Savanna
<i>Panicum parvifolium</i>	Herb	Savanna
<i>Paspalum</i> sp1	Herb	Savanna
Rubiaceae		
<i>Alibertia edulis</i>	Arboreal	Forest
<i>Palicourea</i> sp	Arboreal	Forest

(continued on next page)

Table 1 (continued)

Family and species	Biological form	Veg. units
Sapotaceae		
<i>Pouteria guianensis</i>	Arboreal	Forest
<i>Pouteria</i> sp1	Arboreal	Forest
Selaginellaceae		
<i>Selaginella fragilis</i>	Herb	Savanna
Strelitziaceae		
<i>Phenakospermum guianensis</i>	Arboreal	Forest
Ulmaceae		
<i>Trema micrantha</i>	Arboreal	Forest
Vochysiaceae		
<i>Qualea grandiflora</i>	Arboreal	Forest
<i>Qualea parviflora</i>	Arboreal	Forest
<i>Qualea</i> sp	Arboreal	Forest
<i>Salvertia convallariodora</i>	Arboreal	Forest
<i>Vochysia haenkeana</i>	Arboreal	Forest
<i>Vochysia</i> sp	Arboreal	Forest

600,000 km² that was formed by intraplate extension combined with deformation during the rise of the Andean Chain in the Cretaceous and Tertiary (e.g. Rossetti et al., 2005).

3. Material and methods

3.1. Remote sensing

The morphological aspects of the study area were characterized from analysis of Landsat images 5-TM that were obtained in August 2008 by the Brazilian National Institute for Space Research—INPE. The topographic profile is based on Shuttle Radar Topography Mission-SRTM data. They were acquired from the National Aeronautics and Space Administration—NASA. Global Mapper 8 (Global Mapper LLC, 2009) was used to process the topographic data (Fig. 1).

3.2. Field sampling and sediment description

Ten sediment cores were collected from lowland Amazonia. However, only two cores contained sufficient pollen concentrations for pollen analysis. The sediment cores investigated are located near the towns of Humaitá (HU01, S7° 55' 26"/W63° 04' 59") and Porto Velho (PV02, S8° 46' 43"/W63° 56' 48") ca. 20 km and 0.5 km from the Madeira River, respectively. The Porto Velho site (PV-02) is dominated by dense and open forest, and the Humaitá site (HU-01) presents natural savanna patches surrounded by dense and open forest. The cores were taken from old fluvial terraces that are located about 15 m higher than the modern floodplain on the left margin of the Madeira River (Fig. 1a). Both cores were taken from filled oxbow lakes using a Percussion Drilling System (Hammer Cobra TT). The cores recovered sediment to a depth of 10 and 8 m in a savanna (HU-01) and forest area (PV-02), respectively.

Grain size was determined by laser diffraction using a Laser Particle Size SHIMADZU SALD 2101 in the Laboratory of Chemical Oceanography/UFPB. Prior to grain size analysis, approximately 0.5 g of each sample was immersed in H₂O₂ to remove organic matter, and the residual sediments were disaggregated by ultrasound (França et al., 2012). The grain-size scale of Wentworth (1922) was used in this work with sand (2–0.0625 µm), silt (62.5–3.9 µm) and clay fractions (3.9–0.12 µm). Facies analysis included descriptions of lithology, texture and structures (Harper, 1984; Walker, 1992).

3.3. Palynological analysis

For pollen analysis 1.0 cm³ samples were taken at 5.0 cm intervals in the HU-01 and 20 cm intervals in the PV-02, for a total of 240 samples. All samples were prepared using standard pollen analytical techniques

including acetolysis (Faegri and Iversen, 1989). Sample residues were mounted on slides in glycerin jelly. Pollen and spores were identified by comparison with reference collections of about 4000 Brazilian forest taxa and various pollen keys (Salgado-Labouriau, 1973; Absy, 1975; Markgraf and D'Antoni, 1978; Roubik and Moreno, 1991; Colinvaux et al., 1999), jointly with the reference collections of the Laboratory of Coastal Dynamics—Federal University of Pará and ¹⁴C Laboratory of the Center for Nuclear Energy in Agriculture (CENA/USP) to identify pollen grains and spores. A minimum of 300 pollen grains were usually counted for each sample, but for some specific depths 200 or 250 grains were counted due to their low pollen concentrations. Microfossils consisting of spores, algae and some fungal were also counted, but they were not included in the sum.

Sixty five pollen taxa were identified (Table 3), but the pollen diagrams (Figs. 2 and 3) show only the most abundant pollen taxa (>5% pollen sum) and the different ecological groups defined by Vidotto et al. (2007). The pollen diagrams were statistically subdivided into pollen assemblage zones using a square-root transformation of the percentage data, followed by stratigraphically constrained cluster analysis (Grimm, 1987). The intervals 10–8.6 m and 3.6–0.8 m in core HU-01, and 5.2–0.4 m in core PV-02, exhibit absolute absence of pollen or few pollen grains (<3000 grains/cm³), and these data were not presented in the pollen diagrams.

3.4. Isotopic and chemical analysis

Ninety samples (6–50 mg) were collected at 20 cm intervals from the sediment core, and were treated with 4% HCl to eliminate carbonate, washed with distilled water until pH 6, dried at 50 °C, and finally homogenized. These samples were analyzed for total organic carbon and nitrogen at the Stable Isotope Laboratory of the Center for Nuclear Energy in Agriculture (CENA/USP). The concentration results are expressed in percent of dry weight after the removal of carbonate, with an analytical precision of 0.09 (TOC) and 0.07% (TN). Our C/N data represent the molar ratio between carbon and nitrogen. The organic matter δ¹³C results are expressed as δ¹³C_{org} with respect to VPDB standard, using the following notation:

$$\delta^{13}\text{C}(\text{‰}) = \left[\left(R_{1\text{sample}}/R_{2\text{standard}} \right) - 1 \right] \cdot 1000$$

where $R_{1\text{sample}}$ and $R_{2\text{standard}}$ are the ¹³C/¹²C ratio of the sample and standard. Analytical precision is ± 0.2‰ (Fritz and Fontes, 1980; Hoefs, 1987; Peterson and Fry, 1987; Pessenda et al., 2004).

Different sources of organic matter will be environmentally dependent and will have different δ¹³C and C/N compositions (e.g. Lamb et al., 2006) as follows: C3 terrestrial plants have δ¹³C values between –32‰ and –21‰ and C/N ratios >12, whereas C4 plants have δ¹³C values ranging from –17‰ to –9‰ and C/N ratios >20 (Deines, 1980; Tyson, 1995; Meyers, 1997). Freshwater algae have δ¹³C values between –25‰ and –30‰ (Schidlowski et al., 1983; Meyers, 1997) and marine algae around –24‰ to –16‰ (Haines, 1976; Meyers, 1997). In general, bacteria and algae have C/N ratios of 4–6 and <10, respectively (Meyers, 1997; Tyson, 1995).

3.5. Radiocarbon dating

Based on lithostratigraphic changes, ten samples of sedimentary organic matter (10 g each) were selected for radiocarbon analysis, five in core PV-02 and five in HU-01. In order to avoid contamination by shell fragments, roots and seeds (e.g. Goh, 2006), the sediment samples were examined and physically cleaned under a stereomicroscope. Dating was carried out by BETA Analytic Laboratory using an accelerator mass spectrometer (AMS). Radiocarbon ages were normalized to a δ¹³C of –25‰ VPDB and reported as calibrated years (cal yr B.P.) (2σ) using CALIB 6.0 software and Intcal09 curve (Reimer et al., 2009). The

Table 2
AMS ^{14}C dating of samples derived from sedimentary deposits.

BETA	Core	Depth (m)	$\delta^{13}\text{C}$ (‰)	Measured age (BP)	2 sigma calibration (cal yr B.P.)	Mean calibrated age (cal yr B.P.)
288718	HU01	0.8–0.9	–16.5	6310 ± 40	7317–7163	~7200
288719	HU01	2.6–2.7	–25.1	13,770 ± 60	17,065–16,717	~16,900
285261	HU01	4.0–4.1	–26.6	30,800 ± 170	35,584–34,804	~35,200
304791	HU01	4.6–4.7	–26.8	34,030 ± 200	39,593–38,494	~39,000
288720	HU01	6.7–6.8	–26.0	38,130 ± 360	43,168–42,033	~42,600
288714	PV2	0.65–0.75	–25.3	3050 ± 40	3367–3158	~3250
285259	PV2	3.65–3.70	–25.4	9590 ± 50	11,144–10,741	~11,000
304790	PV2	4.0	–25.1	9700 ± 50	11,231–11,068	~11,150
296243	PV2	6.8–6.9	–28.4	6270 ± 40	7273–7154	~7200
288715	PV2	7.8–8.0	–26.0	9470 ± 50	10,819–10,574	~10,700

sedimentation rates were based on the linear interpolation between age control points.

4. Results

4.1. Radiocarbon dates

Dates of core samples are shown in Table 2 and range from 3367–3158 cal yr B.P. to 43,168–42,033 cal yr B.P. The dates of core HU-01 indicate that its sedimentary deposits accumulated relatively

undisturbed. However, core PV-02 between 7 and 4 m contains age inversions (Fig. 3) that may reflect a rapid filling of the lake during the early Holocene. Alternatively, the two samples between 4 and 3.7 m (Table 2) that are older than the base of this profile may be the products of an eventual reworking of other Holocene sedimentary sequences, as suggested by the difference in grain size around 3.7 m (Fig. 3) that is significantly different from the rest of this stratigraphic profile. Therefore, this age inversion prevents establishing a chronological model that integrates the samples in the 3.7 and 4 m depth with the other dates in core PV-02.

The calculated sedimentation rates in core PV-02 are 0.3 mm/yr (8.0–6.9 m), 1.5 mm/yr (6.9–0.75 m) and 0.2 mm/yr (0.75–0 m), whereas core HU-01 accumulated at rates of 0.6 mm/yr (6.8–4.7 m), 0.2 mm/yr (4.7–4.1 m), 0.1 mm/yr (4.1–2.7 m), 0.2 mm/yr (2.7–0.9 m) and 0.1 mm/yr (0.9–0 m). Although the rates are nonlinear between the dated points, they are of the same order of magnitude as the vertical accretion range of lakes reported by other authors (e.g. Burbridge et al., 2004).

4.2. Facies description

Lakes, tidal flats and fluvial floodplains provide suitable conditions for muddy accumulation and preservation of pollen grains sourced from vegetation living at the time that the sediment was deposited. Lacustrine sediments preserve pollen carried by wind and from vegetation surrounding the lake. The spatial representation of the lacustrine pollen signal depends on wind strengths and the extent of the drainage system feeding the lake. The proportion of the pollen signal provided by each vegetation type is distance-weighted (e.g. Davis, 2000; Xu et al., 2012), with closer sources usually being greater. Tidal-flats and fluvial floodplains collect a smaller spatial representation of vegetation than lacustrine environments, inasmuch as pollen traps in a tidal-plain in Northern Brazil influenced by rivers and colonized by herbaceous vegetation recorded < 1% pollen from mangroves located ~1 km distant (Behling et al., 2001).

The pollen records from active fluvial system reflect a mixture of pollen signals of different rocks/sediments from different times, as the sediment deposited by rivers is a product of reworked material from their margins. In addition, some studies have reported pollen transport in rivers (e.g. Brush and Brush, 1972; Solomon et al., 1982).

Therefore, we consider the pollen studies combined with the facies analysis highly relevant. Pollen and spore records, $\delta^{13}\text{C}_{\text{org}}$ and $\text{C}/\text{N}_{\text{molar}}$ values were interpreted in addition to sedimentological characteristics in order to define four facies that represent the shift from an abandonment channel to a lacustrine environment (Fig. 4).

4.2.1. Active fluvial channel facies (>~42,500 cal yr B.P.)

This facies occurs in core HU-01 between 10 and 8.2 m depth (Fig. 2). It is characterized by fining upward sandy deposits. Pollen grains are absent in this interval. There is an oscillation in total organic carbon (TOC), but with an increasing trend from the bottom (0.1–

Table 3
Pollen taxa identified in the HU-01 and PV-02.

Taxa	Taxa
Aizoaceae	Fabaceae
Amaranthaceae/Chenopodiaceae	<i>Bonara</i>
Amaranthaceae	<i>Copaifera</i>
<i>Gomphrena/Pfaffia</i>	<i>Macrobium</i>
<i>Alternanthera</i>	<i>Myroxylon</i>
Anacardiaceae	<i>Mimosa</i>
<i>Anacardium</i>	Lamiaceae
Annonaceae	<i>Origanum</i>
<i>Annona</i>	Lauraceae
Apocynaceae	Malpighiaceae
Aquifoliaceae	<i>Byrsonima</i>
<i>Ilex</i>	Malvaceae
Araliaceae	Melastomataceae/Combretaceae
<i>Didymopanax</i>	Meliaceae
Arecaceae	Moraceae/Urticaceae
<i>Euterpe</i>	Myristicaceae
<i>Mauritia</i>	<i>Virola</i>
Asteraceae	Myrtaceae
Betulaceae	Nyctaginaceae
<i>Alnus</i>	Onagraceae
Bignoniaceae	Piperaceae
Boraginaceae	<i>Piper</i>
Burseraceae	Poaceae
<i>Protium</i>	Podocarpaceae
Cannabaceae	<i>Podocarpus</i>
<i>Celtis</i>	Polygonaceae
Chloranthaceae	<i>Symmeria</i>
<i>Hedyosmum</i>	Proteaceae
Chrysobalanaceae	<i>Roupala</i>
Clusiaceae	Rubiaceae
<i>Clusia</i>	<i>Alibertia</i>
Connaraceae	<i>Borreria</i>
Convolvulaceae	<i>Psychotria</i>
Cunoniaceae	<i>Spermacoce</i>
<i>Weinmannia</i>	Rutaceae
Cyperaceae	Sapotaceae
Dilleniaceae	Selaginellaceae
<i>Curatella</i>	Tiliaceae
Ericaceae	Winteraceae
Euphorbiaceae	<i>Drymis</i>
<i>Alchornea</i>	
<i>Mabea</i>	
<i>Pachystroma</i>	

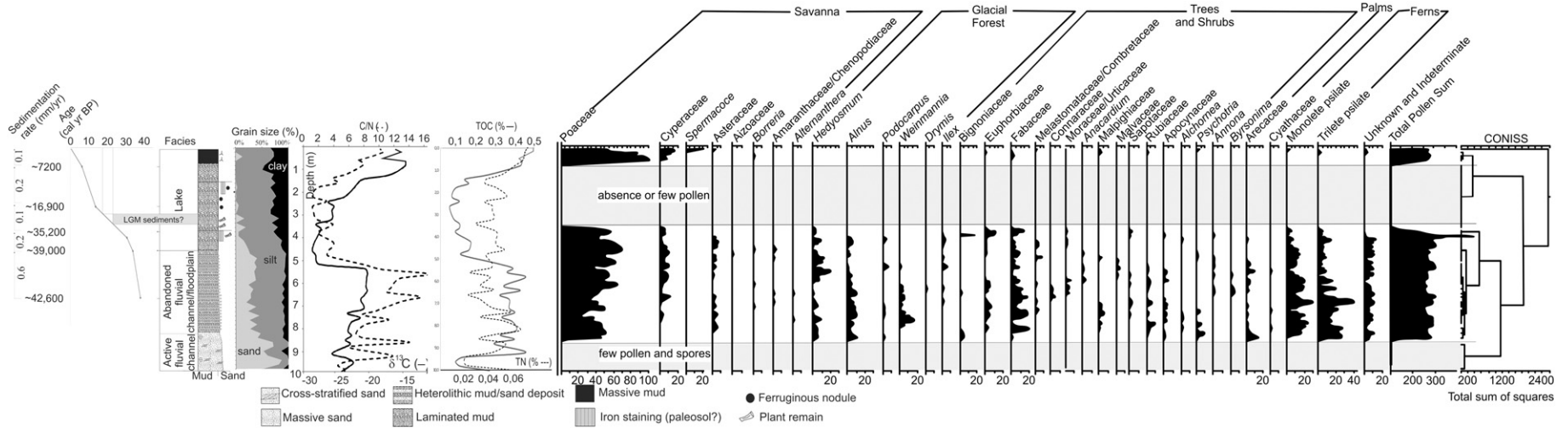


Fig. 2. Sediment core from Humaitá site (HU-01). Sedimentary structure, sediment grain size, organic matter $\delta^{13}\text{C}$ and $\text{C}/\text{N}_{\text{molar}}$ values, summary diagram of pollen proportion for different vegetation groups and proportions of the most frequent pollen taxa.

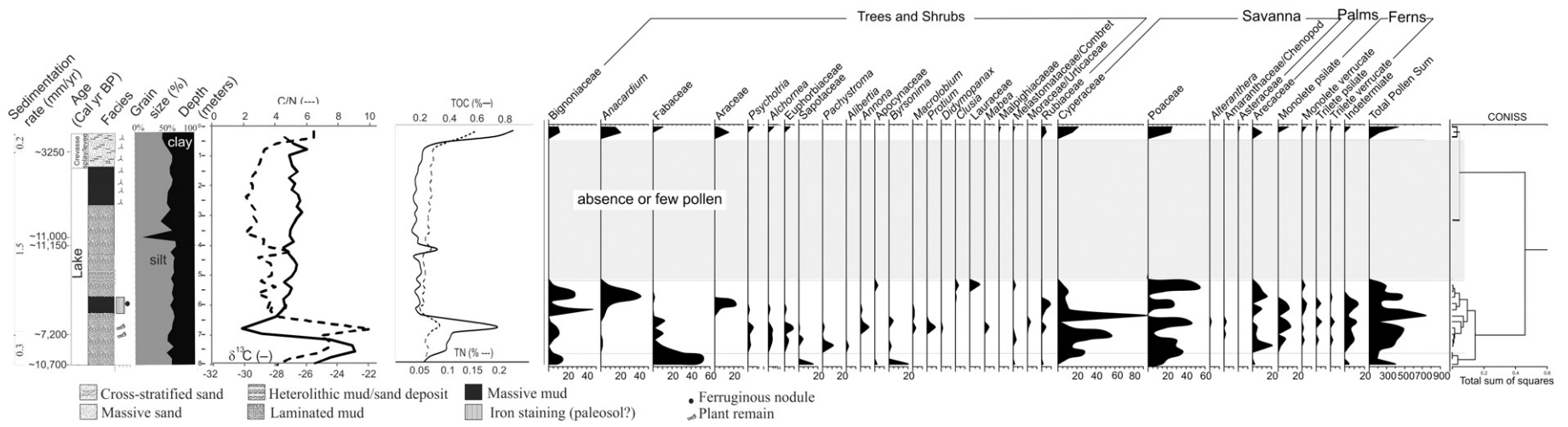


Fig. 3. Pollen records from Porto Velho site (PV02). Sedimentary structure, sediment grain size, organic matter $\delta^{13}\text{C}$ and $\text{C}/\text{N}_{\text{molar}}$ values, summary diagram of pollen proportion for different vegetation groups and proportions of the most frequent pollen taxa.

0.3%) to the top (0.5%) and a slight decrease at 8.4 m depth (0.3%). Total nitrogen (TN) oscillated between 0.02% and 0.06%. $\delta^{13}\text{C}_{\text{org}}$ and $\text{C}/\text{N}_{\text{molar}}$ values range from -25‰ to -23‰ , and from 4.5 to 14, respectively.

4.2.2. Abandoned fluvial channel/floodplain facies (>~42,500 to ~39,000 cal yr B.P.)

This facies occurs in core HU-01 between >~42,600 cal yr B.P. and ~39,000 cal yr B.P. (8.2–4.6 m). The sandy deposits grade upward into heterolithic mud/sand deposits. TOC oscillated between 0.3% and 0.4% with a decrease to 0.1% in 4.8 m. TN oscillated between 0.02% and 0.07%. The $\delta^{13}\text{C}_{\text{org}}$ and $\text{C}/\text{N}_{\text{molar}}$ data show upward increasing trends, with values varying from -23‰ to -20‰ and 7 to 17, respectively. Pollen assemblages are characterized by a slight upward increase in herbs (35–70%) and a decrease in forest components. Herbs are represented by Poaceae (27–63%) and Cyperaceae (0–12%). The modern representative taxa from Amazonian forest pollen (15–35%) consists mainly of Euphorbiaceae (0–10%), Fabaceae (3–20%), Bignoniaceae (0–20%), Sapotaceae (0–3%) and Apocynaceae (0–6%). Pollen components from these sediments also include an assemblage representative of taxa currently found under colder climates (10–27%), such as *Alnus* (2–11%), *Hedyosmum* (2–17%), *Weinmannia* (0–18%), *Podocarpus* (0–4%), *Ilex* (0–4%) and *Drymis* (0–1%). Palm pollen (0–17%) is also present (Fig. 2).

4.2.3. Oxbow lake facies

4.2.3.1. Core HU-01 (~39,000 cal yr B.P. to modern). This facies occurs in the top of core HU-01 from ~39,000 cal yr B.P. until the present (4.6–0 m, Fig. 2). These deposits consist mainly of laminated or massive mud. The transition from abandoned fluvial channel to oxbow lake deposits is marked by a significant decrease in TOC (0.4% to 0.1%), but the TN presents an increasing trend (0.04% to 0.06%). It also shows a drop of $\delta^{13}\text{C}_{\text{org}}$ values (-20‰ to -27‰), followed by a decrease in $\text{C}/\text{N}_{\text{molar}}$ values (17 to 3). During the past ~16,900 cal yr B.P. (2.6–0 m) increases occur in TOC (0.1% to 0.4%) and TN (0.04% to 0.08%), and progressive increases of $\delta^{13}\text{C}_{\text{org}}$ (-27‰ to -14‰) and $\text{C}/\text{N}_{\text{molar}}$ values (2 to 10) occur (Fig. 2).

Between ~39,000 cal yr B.P. and ~35,200 cal yr B.P., pollen data record an expansion of herbs (50–85%), mainly Poaceae (50–75%) and Cyperaceae (6–10%). Representative taxa that occur in Amazon forest today decreased during this phase (5–26%), while taxa currently found under colder climates, represented by *Hedyosmum* (2–20%), *Alnus* (1–7%), *Podocarpus* (0–5%) and *Ilex* (1–9%), remained relatively high (5–23%). An absolute absence of pollen or few pollen grains (<3000 grains/cm³) were recorded between ~35,200 cal yr B.P. and ~7200 cal yr B.P., and are thus not included in the pollen diagram. Since ~7200 cal yr B.P., herbaceous pollen (90–100%), mostly Poaceae (57–100%), Cyperaceae (0–17%), and Asteraceae (0–5%) dominated. This time interval recorded taxa that occur in the savanna today and the absence of taxa currently found under colder climates.

4.2.3.2. Core PV-2 (~10,700 to ~3700 cal yr B.P.). The oxbow lake facies occurs in the lower sections of core PV-02 (8–1.3 m, Fig. 3). It records heterolithic and muddy deposits. The deeper part of this core records a succession that ends in a massive reddish mud. TOC has relatively low values around 0.2% between 6.4 and 0.8 m, but between 8 and 6.8 m an increasing trend from 0.2% to 0.7% occurs. TN values show a weak increasing trend from 8 m until 1.4 m (0.05% to 0.07%). $\delta^{13}\text{C}_{\text{org}}$ and $\text{C}/\text{N}_{\text{molar}}$ values exhibit abrupt changes from -25‰ to -30‰ and 10 to 4, respectively. Younger deposits have $\delta^{13}\text{C}_{\text{org}}$ values around -27‰ , and $\text{C}/\text{N}_{\text{molar}}$ ratios oscillate between 2 and 6 (Fig. 3).

Between 8 and 5.3 m depth, the forest pollen percentage values are between 10 and 55%, being mainly represented by Fabaceae (4–12%), Bignoniaceae (1–11%), Anacardiaceae (0–4%) and Euphorbiaceae (0–10%), and herbs (40–87%) are represented by Cyperaceae (6–90%)

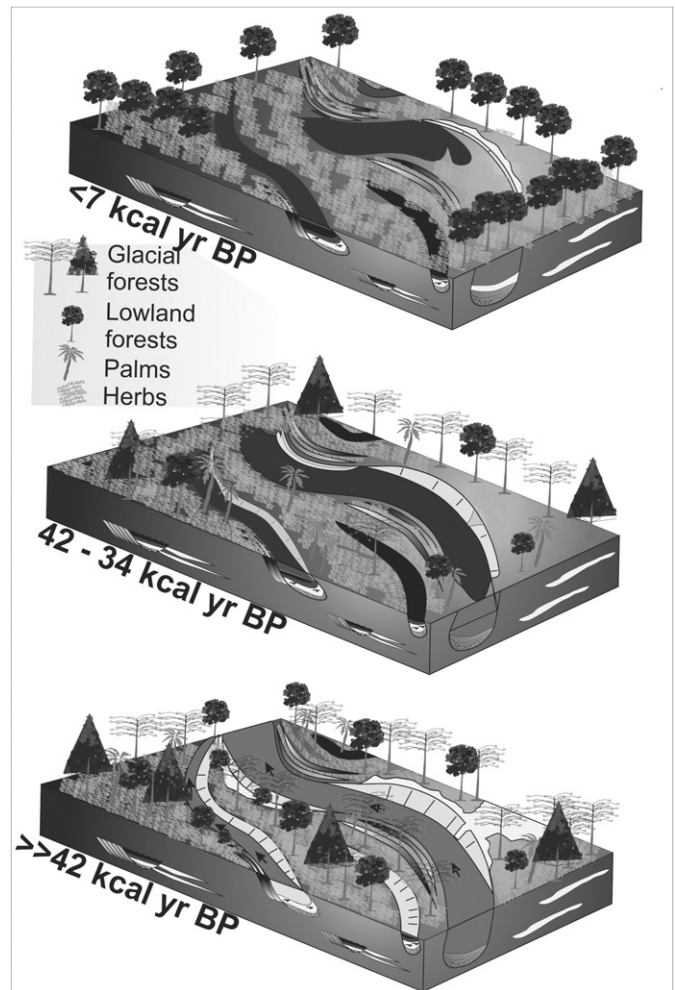


Fig. 4. Geomorphologic and vegetation evolution model for the study site.

and Poaceae (2–50%). In the 6.5–5.3 m interval, the forest pollen percentages increase (55–73%), and, consequently, the herbaceous pollen percentages decrease (15–60%). Pollen grains were absent in the interval between 5.4 m and 0.7 m depth.

4.2.4. Crevasse splay/levee facies (~3700 cal yr B.P. to modern)

This facies occurs only in top of core PV-02 and consists of massive pelite (Fig. 3). TOC and TN values exhibit an increasing trend from 0.2% to 0.8% and 0.07% to 0.16%, respectively. The $\delta^{13}\text{C}_{\text{org}}$ values are between -27.5 and -26‰ , whereas the $\text{C}/\text{N}_{\text{molar}}$ values remain between 5 and 6.3. Since ~3250 cal yr B.P., the forest pollen percentage (55–60%) has higher values than herbaceous (27–42%) and palm pollen (0–11%).

5. Discussion

5.1. Palaeoenvironmental interpretation

The fining upward sandy deposits at the base of core HU-01 (10–8.2 m, Fig. 2) are representative of the active phase of the fluvial channel infilling (Fig. 4). Although pollen grains are absent from this interval, the relation of $\delta^{13}\text{C}_{\text{org}}$ (-25‰ and -23‰) and $\text{C}/\text{N}_{\text{molar}}$ values (4.5–14) suggests that it contains a mixture of organic matter from C₃ plants (macrophytes and flooded vegetation) and freshwater algae.

Between >~42,600 cal B.P. and ~39,000 cal yr B.P. (8.2–4.6 cm), the sandy deposits grade upward into heterolithic mud/sand deposits. This interval is probably related to the gradual abandonment of the fluvial

channel and consequent lake development. $\delta^{13}\text{C}_{\text{org}}$ (–23‰ to –20‰) and $\text{C}/\text{N}_{\text{molar}}$ (7 to 17) data show upward increasing trends, suggesting increased contributions from C_4 plants. Pollen assemblages are consistent with this trend as they are characterized by a slight upward increase in herbs (35–70%). Although the taxa representative of modern Amazonian forest (15–35%) occur during this interval, a significant pollen percentage is from an assemblage representative of taxa currently found under colder climates (10–27%) (Figs. 2 and 4).

Sediments in the upper sections of core HU-01, from ~39,000 cal yr B.P. until the present (4.6–0 cm), correspond to the oxbow lake phase developed after complete channel abandonment (Figs. 2 and 4). The transition from an abandoned fluvial channel to oxbow lake deposits is marked by a significant lowering of $\delta^{13}\text{C}_{\text{org}}$ values (–20‰ to –27‰), followed by a decrease in $\text{C}/\text{N}_{\text{molar}}$ values (17 to 3) caused by the decrease of TOC and increase of TN percentage values (Fig. 2). The depletion of $\delta^{13}\text{C}_{\text{org}}$ and decrease in $\text{C}/\text{N}_{\text{molar}}$ values were probably caused by the relative increase in contribution of organic matter from freshwater algae during the lake establishment. Pollen data showed expansion of herbs (50–85%) between ~39,000 cal yr B.P. and ~35,200 cal yr B.P., with a probable presence of C_3 grasses. Generally, macrophytes in lakes of the Amazon basin present isotopic values typical of C_3 plants (e.g. Zocatelli et al., 2011). Representative taxa that occur in Amazon forest today decreased during this phase (5–26%), while taxa currently found under colder climates remained relatively high (5–23%).

The sediments that accumulated during the LGM did not yield radiocarbon dates. Considering the relative low sedimentation rate (0.1 mm/yr) between ~35,200 and ~16,900 cal yr B.P. and the chronological model proposed for core HU-01 (Fig. 2), a sedimentary hiatus probably occurred in the beginning of the phase having no or few pollen. Ledru et al. (1998) reevaluated pollen records from lowland tropical forests of South America and concluded that probably in none of the published records are LGM sediments present or abundant. This conclusion is based on the occurrence of abrupt lithologic changes coupled with changes in sedimentation rate interpolated from radiocarbon dates. These findings suggest that the LGM was represented probably by a hiatus of several thousand years, indicative of a dry climate.

The progressive increases of $\delta^{13}\text{C}_{\text{org}}$ (–27‰ to –14‰), TOC (0.1 to 0.5), TN (0.02 to 0.07), and $\text{C}/\text{N}_{\text{molar}}$ (2 to 10) values in core HU-01 during the past ~16,900 cal yr B.P. indicate a progressive increased contribution of C_4 plants. This change may be related to a greater influence of C_4 macrophyte communities in the top of the sequence and/or to an increase in the contribution of terrestrial C_4 herbs near the study site. Noteworthy is that few pollen grains were preserved during the late Pleistocene and early Holocene in core HU-01 (Fig. 2) and the early and mid Holocene in core PV-02 (Fig. 3). This feature is probably due to an oxidizing environment that is recorded by laminated mud with iron staining and ferruginous nodules that may be related to a dry period during the early and mid Holocene (e.g. Pessenda et al., 1998; Mayle et al., 2000; Pessenda et al., 2001; Burbridge et al., 2004; Moreira et al., 2012) in distinct locations of the Amazon region. Biogeochemical data from Comprido Lake, eastern Amazonian basin, revealed a dry climate between 10,300 and 7800 cal yr B.P., and a gap in sedimentation due to a complete dryness of the lake occurred between 7800 and 3000 cal yr B.P. (Moreira et al., 2013). This dry event may also have established conditions for post-depositional destruction of pollen grains accumulated during the late Pleistocene, inasmuch as the absence of pollen may be caused by oxidation (Havinga, 1967), which is recorded as ferruginous nodules and iron staining along the absence or few pollen preservation phase (Fig. 2).

The top section of core HU-01, which is characterized by massive mud sediment, is marked by a strong increase of TOC (0.1 to 0.5), TN (0.04 to 0.07), $\delta^{13}\text{C}_{\text{org}}$ (–21‰ to –18‰), and $\text{C}/\text{N}_{\text{molar}}$ (4 to 10) values. The lacustrine environment likely remained completely isolated from the river, at least since ~7200 cal yr B.P., because since this time herbaceous pollen (90–100%) have dominated. This time interval also recorded

low values of taxa that occur in Amazon forest today (0–8%) and an absence of taxa currently found under colder climates. In addition, core PV-02 has a mixture of herbaceous, palm and forest pollen, but no glacial forest pollen preserved in heterolithic and muddy deposits related to the Holocene oxbow lake sedimentation (Fig. 3).

5.2. Transported or local occurrence of *Alnus*?

In Brazil, *Alnus* pollen has been recorded in several studies, but it occurs in low percentages (<4%), even in pollen records of the LGM (Absy, 1979; Colinvaux et al., 1996a; Haberle, 1997; Behling et al., 2004; Macedo, 2009). However, the current study finds a cold pollen assemblage (4–26%) associated with relatively high *Alnus* pollen percentages (2%–11%) between >42,600 cal yr B.P. and <35,200 cal yr B.P. in core HU-01. Because these new data are the first evidence that *Alnus* trees colonized areas of Western Amazonia, at least during the pre-LGM time interval, we consider a discussion about the possible influences of wind and fluvial transport of *Alnus* pollen to the study site especially relevant.

5.2.1. *Alnus* in other pollen records in South America

In southern Peru, *Alnus* pollen values of <2% are almost certainly attributable to long-distance dispersal, whereas its presence at >5% probably indicates the local occurrence of this plant (Weng et al., 2004b). *Alnus* occurs at 4–13% in samples collected above 2300 m, reflecting the abundance of *Alnus* trees in the moist Andean forest belt between 2300 and 2800 m (Weng et al., 2004b; Reese and Liu, 2005). Pollen records from two lakes, one in northeastern lowland Bolivia and the other in southwestern Amazon Basin, report *Alnus* pollen in very low abundance (<0.5%) in recent sediments (Burbridge et al., 2004).

5.2.2. Wind transport

Open vegetation is likely to have a higher proportion of long distance transport pollen rain, but under a relatively closed canopy the pollen rain should indicate local deposition (Weng et al., 2004b; Gosling et al., 2009). Our stratigraphic record during the late Pleistocene showed a denser arboreal vegetation than today, probably growing around a relatively small body of water (<2 km length), similar to those found today in the study site (Fig. 1a). Hence, this setting may have attenuated the possible effectiveness of wind transport. Furthermore, surface winds blow from east to west in this sector of western Amazonia (Satyamurty et al., 2008, Fig. 1a), thus excluding long distance transport of *Alnus* pollen by wind from the Andes to the study site.

5.2.3. Fluvial transport

During the lake phase some influence of Madeira River on the pollen record is possible. However, the fluvial transport of Andean taxa probably did not affect the pollen signal in the study site because core PV-02, which was acquired from an old oxbow lake, contains only modern taxa, such as Cyperaceae (6–90%), Poaceae (2–50%), Fabaceae (4–55%), Bignoniaceae (1–40%), Anacardiaceae (0–40%) and Euphorbiaceae (0–10%) (Fig. 3) in its Holocene sequence, whereas core HU-01 contains mainly Poaceae (57–100%), Cyperaceae (0–17%), Spermatoceae (0–20%) and Asteraceae (0–5%) during the past ~7200 cal yr B.P. (Fig. 2).

Naturally, a certain percentage of *Alnus* pollen (<5%, Weng et al., 2004b) transported from Andean areas by rivers cannot be completely ruled out. However, considering the relatively high percentages of cold (4–26%) and *Alnus* pollen (2%–11%) between >42,600 cal yr B.P. and <~35,200 cal yr B.P. and their absence from the Holocene section of cores PV-02 (15 samples) and HU-01 (14 samples), *Alnus* likely populated the Western Amazonia lowlands during the pre-LGM time due to cooler temperatures.

5.3. Glacial pollen elements in lowland Amazonia

Modern biogeographic data indicate that *Alnus* occurs along the Andes and Central American mountains at about 2000–3000 m from southern Mexico to 28°S in northwest Argentina (Fig. 1a). In South America, it covers whole mountainsides where mean annual temperatures are between 8 and 18 °C and minimum winter temperatures are no lower than –10 °C (Furrow, 1979; Weng et al., 2004b; Punyasena et al., 2011).

Considering our palaeorecords, the lowland Amazonia between >~42,600 cal yr B.P. and <~35,200 cal yr B.P. was probably dominated by a mixture of both upper montane and lowland elements. Upper montane taxa include *Weinmannia*, *Hedyosmum*, *Alnus*, *Podocarpus*, *Ilex* and *Drymis*, which are virtually absent from the Holocene (Figs. 2 and 3) and modern pollen assemblages (Table 1). Taxa characteristic of lowland vegetation such as *Anacardium*, *Alchornea*, *Psychotria*, *Annona* and *Byrsonima* are represented in the Holocene forest (Fig. 3). Apart from fairly well defined upper montane and lowland taxa, a significant abundance of persistent elements such as Poaceae, Cyperaceae, Fabaceae, Melastomataceae/Combretaceae and Moraceae/Urticaceae is recorded throughout the glacial and in the Holocene pollen assemblages. Reconstructing vegetation from these pollen types is therefore challenging, and it is difficult to interpret unequivocally the climatic significance of these assemblages. Nevertheless, the abundance of highland taxa between >43 kcal yr B.P. and <35 kcal yr B.P. and the absence of montane elements from the Holocene pollen assemblage indicate significant distinction between glacial and Holocene vegetation at the studied site.

With respect to the *Ilex* pollen recorded in core HU-01 during the late Pleistocene, several species of *Ilex* that are common in swamp forest communities occur today in *Mauritia* palm swamps of lowland abandoned channels of Western Amazonia (Roucouxa et al., 2013). However, *Ilex* was not found currently in our study region (Vidotto et al., 2007, Table 1), and *Ilex* pollen was not recorded during the Holocene phase in our record (Fig. 3). The presence of *Ilex* with the pollen assemblage representative of taxa currently found in colder climates should suggest that this species of *Ilex* in our record is adapted to cold climate (e.g. Colinvaux et al., 1996a, 1996b; van der Hammen and Hooghiemstra, 2000; Ledru et al., 2001; D'Apolito et al., 2013).

Given that the glacial Pleistocene assemblage formed by *Weinmannia*, *Hedyosmum*, *Podocarpus*, *Ilex* and *Drymis* is well represented by pollen types that are relatively less dispersed and/or produced in low quantities relative to *Alnus* pollen (Weng et al., 2004b), at least suggests that cold-adapted plants (*Weinmannia*, *Hedyosmum*, *Podocarpus*, *Ilex* and *Drymis*) were occupying terraces near the lakes and zones topographically higher than fluvial plains in the study site. *Alnus* was likely inhabiting the Western Amazonia lowland, but it may have occupied zones comparatively more distant from the study site. Its terrain was not subject to flood influence, inasmuch as these taxa are generally not found in floodplain environments. This cold-climate forest probably colonized areas of the Western Amazonia lowland close enough to the study site to allow the dispersal of their pollen grains and their preservation in lakes and floodplains sediments of the Humaitá region.

5.4. Palaeoclimatic implications of local occurrence of *Alnus*

Palaeoecological studies indicate a cooling (5–9 °C) in the lowland Amazonian rain forest during the LGM (e.g. Bush et al., 2004). Considering that the current mean annual temperature is between 24 °C and 26 °C (Brasil, 1978) at the study site, which is located 1100 km from the foot of the Andes (Fig. 1b), and that *Alnus* occurs in areas with mean annual temperatures between 8 and 18 °C (e.g. Furrow, 1979; Weng et al., 2004a), the local occurrence of *Alnus* calls for a significant decrease in mean annual temperature during the onset of the LGM, at least in this sector of Western Amazonia, to allow the downslope expansion into the lowland rain forest of significant populations of plants

more adapted to cold temperatures. The 1100 km of horizontal and 2000 m of vertical relocation within a time scale of thousands of years is plausible for Andean trees to colonize the lowlands in response to cooling temperature (Feeley et al., 2011).

Pollen studies suggest that polar air influenced the climate and vegetation of the Brazilian Amazon forest during the Late Quaternary, with the expansion of *Podocarpus* and other montane elements into the lowland forest (e.g. Ledru, 1993; Ledru et al., 1994; Colinvaux et al., 1996a; De Oliveira, 1996; Haberle and Maslin, 1999; Colinvaux et al., 2000; Ledru et al., 2001). However, pollen records from the southern margin of Amazonia in eastern Bolivia (750 km away from HU-01), indicate that savanna communities dominated the catchment of this site continuously from 43,000 to 2240 cal yr B.P. Another core, also from eastern Bolivia (650 km away from core HU-01), records mainly *Alchornea*, Leguminosae (Papilionoideae), and *Talisia*-type pollen between ~47,000 and ~43,000 cal yr B.P. All three taxa include species present in the Amazonian rain forest, Cerrado (upland grassland, savanna, and woodland), and Chiquitano dry forest biotas. No sedimentation occurred at this site during the LGM (Mayle et al., 2000).

Today's moisture sources along the eastern slope of the Andes are the tropical Atlantic and the Amazon River basin (Martin et al., 1997). By contrast, snowfall in Bolivia is dependent on winter precipitation related to polar air outbreaks (Vuille and Amman, 1997). The observed difference in moisture and temperature changes between Bolivia and the Brazilian Amazon during the LGM may reflect latitudinal precipitation and temperature gradients. Cold air was brought as far north as the equator. This mechanism explains the observed vegetation changes in Amazonia, which would be related to increased penetration of cold air as represented by the Mobile Polar High concept of Leroux (1993). The present findings are also in good agreement with Rind's models, in which changes in latitudinal temperature gradient affect large-scale atmospheric dynamics (Rind, 2000).

Although our data represent the onset of the LGM (~42,600 cal yr B.P. and ~35,200 cal yr B.P.), which probably was not as cold as the LGM (in the Titicaca region the LGM is defined as 26,000–22,000 cal yr B.P., Weng et al., 2006), the maximum glacier extension was earlier than 24,000 cal yr B.P. in the central Andes (Klein et al., 1998). Terminal moraines were dated (Smith et al., 2005) at their lowest elevation in Bolivia at ~34,000 cal yr B.P., and deglaciation began between 21,000 and 19,000 cal yr B.P. (Seltzer et al., 2002). The climate warmed progressively in many high montane locations between ~20,000 and 18,000 cal yr B.P. (Seltzer et al., 2002; Paduano et al., 2003; Bush et al., 2005).

6. Conclusions

The present study describes sedimentary deposits representative of active channel (>42,000 cal yr B.P.), abandoned channel/floodplain (>~42,600 to ~39,000 cal yr B.P.), and oxbow lake sedimentary environments (~39,000 cal yr B.P. to modern). In these settings, reducing and low energy subaqueous conditions were developed, locally favoring preservation of a pollen assemblages made up initially of herbaceous vegetation, some modern representative taxa from the Amazon forest, and cold-adapted plants (4–26%) from the Andes, represented by *Alnus* (2–11%), *Hedyosmum* (2–17%), *Weinmannia* (0–18%), *Podocarpus* (0–4%), *Ilex* (0–4%) and *Drymis* (0–1%) at least between >~42,600 cal yr B.P. and <~35,200 cal yr B.P. The herbaceous vegetation and modern representative taxa from Amazonian forest persisted through the Holocene, while the cold pollen assemblage became absent. Considering the relative abundance of *Alnus* during the late Pleistocene (core HU-1) compared to Holocene succession (core PV-2) and modern surface samples, the *Alnus* probably populated the Western Amazonia lowland, or it was growing closer to the study site due to cooler temperatures during glacial times.

Acknowledgments

This work is part of the research projects CNPq # 471483/06-0 and CNPq # 550331/2010-7. The authors acknowledge the logistic support provided by the Brazilian Geological Survey-CPRM and the Santo Antonio Hydroelectric during field campaigns. The authors thank the three reviewers for their many constructive comments.

References

- Absy, M.L., 1975. Polen e esporos do Quaternário de Santos (Brasil). *Hoehnea* 5, 1–26.
- Absy, M.L., 1979. A Palynological Study of Holocene Sediments in the Amazon Basin. University of Amsterdam (PhD Thesis).
- Anhuf, D., Ledru, M.-P., Behling, H., Da Cruz Jr, F.W., Cordeiro, R.C., Van Der Hammen, T., Karmann, I., Marengo, J.A., De Oliveira, P.E., Pessenda, L., Sifeddine, A., Albuquerque, A.L., Da Silva Dias, P.L., 2006. Paleo-environmental change in Amazonian and African rainforest during the LGM. *Palaeogeogr. Palaeoclimatol. Palaeoecol.* 239, 510–527.
- Behling, H., 1996. First report on new evidence for the occurrence of *Podocarpus* and possible human presence at the mouth of the Amazon during the Late-glacial. *Veg. Hist. Archaeobot.* 3, 241–246.
- Behling, H., Berrio, J.C., Hooghiemstra, H., 1999. Late Quaternary pollen records from the middle Caqueta river basin in central Colombian Amazon. *Palaeogeogr. Palaeoclimatol. Palaeoecol.* 145, 193–213.
- Behling, H., Cohen, M.C.L., Lara, R.J., 2001. Studies on Holocene mangrove ecosystem dynamics of the Bragança Peninsula in north-eastern Pará, Brazil. *Palaeogeogr. Palaeoclimatol. Palaeoecol.* 167, 225–242.
- Behling, H., Cohen, M.C.L., Lara, R.J., 2004. Late Holocene mangrove dynamics of the Marajó Island in northern Brazil. *Veg. Hist. Archaeobot.* 13, 73–80.
- Brasil, 1978. Projeto RADAMBRASIL. Folha SB.20 Purus; geologia, geomorfologia, pedologia, vegetação e uso potencial da terra. Departamento Nacional de Produção Mineral, Rio de Janeiro.
- Brush, G.S., Brush, L.M.J., 1972. Transport of pollen in a sediment laden channel: a laboratory study. *Am. J. Sci.* 272, 359–381.
- Burbridge, R.E., Mayle, F.E., Killeen, T.J., 2004. Fifty-thousand-year vegetation and climate history of Noel Kempff Mercado National Park, Bolivian Amazon. *Quat. Res.* 61, 215–230.
- Bush, M.B., 1994. Amazonian speciation: a necessarily complex model. *J. Biogeogr.* 21, 5–18.
- Bush, M.B., 2002. Distributional change and conservation on the Andean flank: a palaeoecological perspective. *Glob. Ecol. Biogeogr.* 11, 463–467.
- Bush, M.B., Colinvaux, P.A., Wiemann, M.C., Piperno, D.R., Liu, K., 1990. Late Pleistocene temperature depression and vegetation change in Ecuadorian Amazonia. *Quat. Res.* 34, 330–345.
- Bush, M.B., Piperno, D.R., Colinvaux, P.A., De Oliveira, P.E., Kriesek, L.A., Miller, M.C., Rowe, W.E., 1992. A 14,300-yr palaeoecological profile of a lowland tropical lake in Panama. *Ecol. Monogr.* 62, 251–275.
- Bush, M.B., Silman, M.R., Urrego, D.H., 2004. 48,000 years of climate and forest change in a biodiversity hot spot. *Science* 303, 827–829.
- Bush, M.B., Hansen, B.C.S., Rodbell, D., Seltzer, G.O., Young, K.R., León, B., Silman, B.M.R., Abbott, M.B., 2005. A 17,000-year history of Andean climate and vegetation change from Laguna de Chochos, Peru. *Gosling, J. Quat. Sci.* 20, 703–714.
- Cheng, H., Sinha, A., Cruz, F.W., Wang, X., Edwards, R.L., D'horta, F.M., Ribas, C.C., Vuille, M., Stott, L.D., Auler, A.S., 2013. Climate change patterns in Amazonia and biodiversity. *Nat. Commun.* 4 (1411), 2013.
- Colinvaux, P.A., 1998. A new vicariance model for Amazonian endemics. *Glob. Ecol. Biogeogr. Lett.* 7, 95–96.
- Colinvaux, P.A., De Oliveira, P.E., Moreno, J.E., Miller, M.C., Bush, M.B., 1996a. A long pollen record from lowland Amazonia: forest and cooling in glacial times. *Science* 247, 85–88.
- Colinvaux, P.A., Liu, K., De Oliveira, P.E., Bush, M.B., Miller, M.C., Steinitz-Kannan, M., 1996b. Temperature depression in the lowland tropics in glacial times. *Clim. Chang.* 32, 19–33.
- Colinvaux, P.A., Bush, M.B., Steinitz-Kannan, M., Miller, M.C., 1997. Glacial and post-glacial pollen records from the Ecuadorian Andes and Amazon. *Quat. Res.* 48, 69–78.
- Colinvaux, P., De Oliveira, P.E., Patiño, J.E.M., 1999. Amazon Pollen Manual and Atlas. Harwood Academic Publishers, Dordrecht (332 pp.).
- Colinvaux, P.A., De Oliveira, P.E., Bush, M.B., 2000. Amazonian and neotropical plant communities on glacial time-scales: the failure of the aridity and refuge hypothesis. *Quat. Sci. Rev.* 19, 141–169.
- Cordeiro, R.C., Turcq, B.J., Sifeddine, A., Lacerda, L.D., Silva Filho, E.V., Gueiros, B.B., Cunha, Y.P.P., Santelli, R.E., Pádua, E.O., Pachinelam, S.R., 2011. Biogeochemical indicators of environmental changes from 50 ka to 10 ka. *Palaeogeogr. Palaeoclimatol. Palaeoecol.* 299, 426–436.
- Cottam, G., Curtis, J.T., 1956. The use of distance measure in phytosociological sampling. *Ecology* 37, 451–460.
- D'Apolito, C., Absy, M.L., Latrubessec, E.M., 2013. The Hill of Six Lakes revisited: new data and re-evaluation of a key Pleistocene Amazon site. *Quat. Sci. Rev.* 76, 140–155.
- Davis, M.B., 2000. Palynology after Y2K—understanding the source area of pollen in sediments. *Annu. Rev. Earth Planet. Sci.* 28, 1–18.
- De Oliveira, P.E., 1992. A Palynological Record of Late Quaternary Vegetation and Climatic Change in Southeastern Brazil. Ohio State University, Columbus, OH (Ph.D. Thesis).
- De Oliveira, P.E., 1996. Glacial cooling and forest disequilibrium in western Amazonia. *Acad. Bras. Cienc.* 68, 129–138.
- Deines, P., 1980. The isotopic composition of reduced organic carbon. In: Fritz, P., Fontes, J.C. (Eds.), *Handbook of Environmental Isotope Geochemistry. The Terrestrial Environment*, vol. 1. A. Elsevier, Amsterdam, pp. 329–406.
- Faegri, K., Iversen, J., 1989. *Textbook of Pollen Analysis*. Wiley, J., Sons, X, New York.
- Feeley, K.J., Silman, M.R., Bush, M.B., Farfan, W., Cabrera, K.G., Malhi, Y., Meir, P., Revilla, N.S., Quisipyanqui, M.N.R., Saatchi, S., 2011. Upslope migration of Andean trees. *J. Biogeogr.* 38, 783–791.
- França, M.C., Francisquini, M.I., Cohen, M.C.L., Pessenda, L.C.R., Rossetti, D.F., Guimarães, J.T.F., Smith, C.B., 2012. The last mangroves of Marajó Island Eastern Amazon: impact of climate and/or relative sea-level changes. *Rev. Palaeobot. Palynol.* 187, 50–65.
- Fritz, P., Fontes, J.C.H., 1980. In: Fritz, P., Fontes, J.C.H. (Eds.), *Handbook of Environmental Isotope Geochemistry*. Elsevier, Amsterdam, pp. 1–17.
- Furlow, J.J., 1979. The systematics of the American species of *Alnus* (Betulaceae). *Rhodora* 81, 1–121.
- Global Mapper LLC, 2009. Global Mapper Version 9.0 Software. (Colorado, Parker).
- Goh, K.M., 2006. Removal of contaminants to improve the reliability of Radiocarbon dates of peats. *J. Soil Sci.* 29, 340–349.
- Gosling, W.D., Mayle, F.E., Tate, N.J., Killeen, T.J., 2009. Differentiation between neotropical rainforest, dry forest, and savanna ecosystems by their modern pollen spectra and implications for the fossil pollen record. *Rev. Palaeobot. Palynol.* 153, 70–85.
- Grimm, E.C., 1987. CONISS: a Fortran 77 program for stratigraphically constrained cluster analysis by the method of the incremental sum of squares. *Pergamon J.* 13, 13–35.
- Guilderson, T.P., Fairbanks, R.G., Rubenstone, J.L., 1994. Tropical temperature variations since 20,000 years ago: modulating interhemispheric climate change. *Science* 263, 663–665.
- Haberle, S.G., 1997. Upper Quaternary vegetation and climate history of the Amazon basin: correlating marine and terrestrial pollen records. In: Flood, R.D., Piper, D.J.W., Klaus, A., Peterson, L.C. (Eds.), *Proceedings of the Ocean Drilling Program, Scientific Results*, vol. 155, pp. 381–396 (College Station, TX).
- Haberle, S.G., Maslin, M.A., 1999. Late Quaternary vegetation and climate change in the Amazon Basin on a 50,000 year pollen record from the Amazon fan, ODP Site 932. *Quat. Res.* 51, 27–38.
- Haines, E.B., 1976. Stable carbon isotope ratios in biota, soils and tidal water of a Georgia salt marsh. *Estuar. Coast. Mar. Sci.* 4, 609–616.
- Harper, C.W., 1984. Improved methods of facies sequence analysis. In: Walker, R.G. (Ed.), *Facies Models 2ed*. Geological Association of Canada, Ontario, pp. 11–13.
- Havinga, A.J., 1967. Palynology and pollen preservation. *Rev. Palaeobot. Palynol.* 2, 81–98.
- Hoefs, J., 1987. *Stable Isotope Geochemistry*. Springer-Verlag, Berlin 201.
- Irion, G., 1982. Mineralogical and geochemical contribution to climatic history in central Amazonia during Quaternary time. *Trop. Ecol.* 23, 76–85.
- Klein, A.G., Seltzer, G.O., Isacks, B.L., 1998. Modern and local glacial maximum snowlines in the central Andes of Peru, Bolivia and Northern Chile. *Quat. Sci. Rev.* 17, 1–21.
- Lamb, A.L., Wilson, G.P., Leng, M.J., 2006. A review of coastal palaeoclimate and relative sea-level reconstructions using $\delta^{13}C$ and C/N ratios in organic material. *Earth Sci. Rev.* 75, 29–57.
- Latrubesse, E.M., 2002. Evidence of Quaternary palaeohydrological changes in middle Amazônia: the Aripuanã–Roosevelt and Jiparaná fans. *Z. Geomorphol.* 129, 61–72.
- Ledru, M.P., 1993. Late Quaternary environmental and climatic changes in central Brazil. *Quat. Res.* 39, 90–98.
- Ledru, M.-P., Behling, H., Fournier, M., Martin, L., Servant, M., 1994. Localisation de la forêt d'Araucaria du Brésil au cours de l'Holocène. Implications paléoclimatiques. *C. R. Acad. Sci. Paris* 317, 517–521.
- Ledru, M.P., Bertaux, J., Sifeddine, A., 1998. Absence of Last Glacial Maximum records in lowland tropical forests. *Quat. Res.* 49, 233–237.
- Ledru, M.P., Cordeiro, R.C., Dominguez, J.M.L., Martin, L., Mourguiart, P., Sifeddine, A., Turcq, B., 2001. Late-glacial cooling in Amazonia as inferred from pollen at Lagoa do Caçó, Northern Brazil. *Quat. Res.* 55, 47–56.
- Leroux, M., 1993. The Mobile Polar High: a new concept explaining present mechanisms of meridional air-mass and energy exchanges and global propagation of palaeoclimatic changes. *Glob. Planet. Chang.* 7, 69–93.
- Liu, K.-B., Colinvaux, P.A., 1985. Forest changes in the Amazon basin during the last glacial maximum. *Nature* 318, 556–557.
- Macedo, R.B., 2009. Análise palinológica de um testemunho holocênico em Santo Antônio da Patrulha, Rio Grande do Sul, Brasil. Federal University of Rio Grande do Sul, Brazil (Master Thesis).
- Markgraf, V., D'Antoni, H.L., 1978. *Pollen Flora of Argentina*. University of Arizona Press, Tucson.
- Martin, L., Bertaux, J., Correge, T., Ledru, M.-P., Mourguiart, P., Sifeddine, A., Soubies, F., Wirmann, D., Suguio, K., Turcq, B., 1997. Astronomical forcing of contrasting rainfall changes in tropical South America between 12,400 and 8800 cal yr B.P. *Quat. Res.* 47, 117–122.
- Mayle, F.E., Burbridge, R., Killeen, T.J., 2000. Millennial-scale dynamics of Southern Amazonian rain forests. *Science* 290, 2291–2294.
- Meyers, P.A., 1997. Organic geochemical proxies of paleoceanographic, paleolimnologic and paleoclimatic processes. *Org. Geochem.* 27, 213–250.
- Moreira, L.S., Moreira-Turcq, P., Turcq, B., Caquineau, S., Cordeiro, R.C., Turcq, B., 2012. Paleohydrological changes in an Amazonian floodplain lake: Santa Ninha Lake. *J. Paleolimnol.* 48, 339–350.
- Moreira, L.S., Moreira-Turcq, P., Cordeiro, R.C., Turcq, B., Caquineau, S., Viana, J.C.C., Brandini, N., 2013. Holocene paleoenvironmental reconstruction in the Eastern Amazonian Basin: Comprido Lake. *J. S. Am. Earth Sci.* 44, 55–62.
- Mosblech, N.A.S., Bush, M.B., Gosling, W.D., Hodell, D., Thomas, L., Van Calsteren, P., Correa-Metrio, A., Valencia, B.G., Curtis, J., Van Woesik, R., 2012. North Atlantic forcing of Amazonian precipitation during the Last Ice Age. *Nat. Geosci.* 5, 817–820.

- Mourguiart, P., Ledru, M.P., 2003. Last Glacial Maximum in an Andean cloud forest environment (Eastern Cordillera, Bolivia). *Geology* 31, 195–198.
- Paduano, G.M., Bush, M.B., Baker, P.A., Fritz, S.C., Seltzer, G.O., 2003. A vegetation and fire history of Lake Titicaca since the Last Glacial Maximum. *Palaeogeogr. Palaeoclimatol. Palaeoecol.* 194, 259–279.
- Pessenda, L.C.R., Gomes, B.M., Aravena, R., Ribeiro, A.S., Boulet, R., Gouveia, S.E.M., 1998. The carbon isotope record in soils along a forest-cerrado ecosystem transect: implications for vegetation changes in the Rondônia state, southwestern Brazilian Amazon region. *The Holocene* 8, 599–603.
- Pessenda, L.C.R., Boulet, R., Aravena, R., Rosolen, V., Gouveia, S.E.M., Ribeiro, A.S., Lamote, M., 2001. Origin and dynamics of soil organic matter and vegetation changes during the Holocene in a forest-savanna transition zone, Brazilian Amazon region. *The Holocene* 11, 250–254.
- Pessenda, L.C.R., Ribeiro, A.S., Gouveia, S.E.M., Aravena, R., Boulet, R., Bendassoli, J.A., 2004. Vegetation dynamics during the late Pleistocene in the Barreirinhas region, Maranhão State, northeastern Brazil, based on carbon isotopes in soil organic matter. *Quat. Res.* 62, 183–193.
- Pessenda, L.C.R., De Oliveira, P.E., Mofatto, M., De Medeiros, V.B., Garcia, R.J.F., Aravena, R., Bendassoli, J.A., Leite, A.Z., Saad, A.R., Etchebehere, M.L., 2009. The evolution of a tropical rainforest/grassland mosaic in Southeastern Brazil since 28,000 ¹⁴C yr BP based on carbon isotopes and pollen records. *Quat. Res.* 71, 437–452.
- Peterson, B.J., Fry, B., 1987. Stable isotope in ecosystem studies. *Annu. Rev. Ecol. Syst.* 18, 292–320.
- Punyaseena, S.W., Dalling, J.W., Jaramillo, C., Turner, B.J., 2011. Comment on “The response of vegetation on the Andean flank in western Amazonia to Pleistocene climate change”. *Science* 333, 1825.
- Räsänen, M., Salo, J., Kalliola, R., 1987. Fluvial perturbation in the western Amazon basin: regulation by long term sub-Andean tectonics. *Science* 238, 1398–1401.
- Reese, C.A., Liu, K., 2005. A modern pollen rain study from the central Andes region of South America. *J. Biogeogr.* 32, 709–718.
- Reimer, P.J., Baillie, M.G.L., Bard, E., Bayliss, A., Beck, J.W., Blackwell, P.G., Bronk Ramsey, C., Buck, C.E., Burr, G.S., Edwards, R.L., Friedrich, M., Grootes, P.M., Guilderson, T.P., Hajdas, I., Heaton, T.J., Hogg, A.G., Hughen, K.A., Kaiser, K.F., Kromer, B., McCormac, F.G., Manning, S.W., Reimer, R.W., Richards, D.A., Southon, J.R., Talamo, S., Turney, C.S.M., Van der Plicht, J., Weyhenmeyer, C.E., 2009. IntCal09 and Marine09 radiocarbon age calibration curves, 0–50,000 years cal BP. *Radiocarbon* 51, 1111–1150.
- Rind, D., 2000. Relating paleoclimate data and past temperature gradients: some suggestive rules. *Quat. Sci. Rev.* 19, 381–390.
- Rossetti, D.F., Toledo, P.M., Góes, A.M., 2005. New geological framework for Western Amazonia (Brazil) and implications for biogeography and evolution. *Quat. Res.* 63, 78–89.
- Roubik, D.W., Moreno, J.E., 1991. Pollen and Spores of Barro Colorado Island. 36. Missouri Botanical Garden, St. Louis 268.
- Roucoux, K.H., Lawson, I.T., Jones, T.D., Bakera, T.R., Honorio Coronado, E.N., Gosling, W.D., Lähteenoja, O., 2013. Vegetation development in an Amazonian peatland. *Palaeogeogr. Palaeoclimatol. Palaeoecol.* 374, 242–255.
- Salgado-Labouriau, M.L., 1973. Contribuição à palinologia dos cerrados. *Academia Brasileira de Ciências, Rio de Janeiro* (273 pp.).
- Salo, J., 1987. Pleistocene forest refuges in the Amazon: evaluation of the biostratigraphical, lithostratigraphical and geomorphological data. *Ann. Zool. Fenn.* 24, 203–211.
- Satyamurthy, P., Sousa Jrl., S.B., Teixeira, M.S., Silva, L.M.E.G., 2008. Regional circulation differences between a rainy episode and a nonrainy episode in eastern São Paulo State in March 2006. *Rev. Bras. Meteorol.* 23, 404–416.
- Schidlowski, M., Hayes, J.M., Kaplan, I.R., 1983. Isotopic inferences of ancient biochemistries: carbon, sulphur, hydrogen and nitrogen. In: Scholf, J.W. (Ed.), *Earth's Earliest Biosphere, Its Origin and Evolution*. Princeton University Press, Princeton, pp. 149–186.
- Seltzer, G.O., Rodbell, D.T., Baker, P.A., Fritz, S.C., Tapia, P.M., Rowe, H.D., Dunbar, R.B., 2002. Early deglaciation in the tropical Andes. *Science* 298, 1685–1686.
- Smith, J.A., Seltzer, G.O., Farber, D.L., Rodbell, D.T., Finkel, R.C., 2005. Early local Last Glacial Maximum in the tropical Andes. *Science* 308, 678–681.
- Solomon, A.M., Blasing, T.J., Solomon, J.A., 1982. Interpretation of floodplain pollen in alluvial sediments from an arid region. *Quat. Res.* 18, 52–71.
- Stute, M., Forster, M., Frischkorn, H., Serejo, A., Clark, J.F., Schlosser, P., Broecker, W.S., Bonani, G., 1995. Cooling of tropical Brazil (5 °C) during the last glacial maximum. *Science* 269, 379–383.
- Thompson, L.G., Davis, M.E., Thompson, E.M., Sowers, T.A., Henderson, K.A., Zagorodnov, V.S., Lin, P.N., Mikhalenko, V.N., Campen, R.K., Bolzan, J.F., Cole-Dai, J., Francou, B., 1998. A 25,000 year tropical climate history from Bolivian ice cores. *Science* 282, 1858–1864.
- Tyson, R.V., 1995. *Sedimentary Organic Matter: Organic Facies and Palynofacies*. Chapman and Hall, London (15 pp.).
- Urrego, D.H., Silman, M.R., Bush, M.B., 2005. The last glacial maximum: stability and change in a western Amazonian cloud forest. *J. Quat. Sci.* 20, 693–701.
- Urrego, D.H., Bush, M.B., Silman, M.R., 2010. A long history of cloud and forest migration from lake Consuelo, Peru. *Quat. Res.* 73, 364–373.
- van der Hammen, T., Absy, M.L., 1994. Amazonia during the last glacial. *Palaeogeogr. Palaeoclimatol. Palaeoecol.* 109, 247–261.
- van der Hammen, T., Hooghiemstra, H., 2000. Neogene and Quaternary history of vegetation, climate and plant diversity in Amazonia. *Quat. Sci. Rev.* 19, 725–742.
- Vidotto, E., Pessenda, L.C.R., Ribeiro, A.S., Freitas, H.A., Bendassoli, J.A., 2007. Dinâmica do ecótono floresta-campo no sul do estado do Amazonas no Holoceno, através de estudos isotópicos e fitossociológicos. *Acta Amazon.* 37, 385–400.
- Vuille, M., Amman, C., 1997. Regional snowfall patterns in the high, arid Andes. *Clim. Chang.* 36, 413–423.
- Walker, R.G., 1992. Facies, facies models and modern stratigraphic concepts. In: Walker, R.G., James, N.P. (Eds.), *Facies Models—Response to Sea Level Change*. Geological Association of Canada, Ontario, pp. 1–14.
- Weng, C., Bush, M.B., Chepstow-Lusty, A.J., 2004a. Holocene changes of Andean alder (*Alnus acuminata*) in highland Ecuador and Peru. *J. Quat. Sci.* 19, 685–691.
- Weng, C., Bush, M.B., Silman, M.R., 2004b. An analysis of modern pollen rain on an elevational gradient in southern Peru. *J. Trop. Ecol.* 20, 113–124.
- Weng, C., Hooghiemstra, H., Duivenvoorden, J., 2006. Challenges in estimating past plant diversity from fossil pollen data: statistical assessment, problems, and possible solutions. *Divers. Distrib.* 12, 310–318.
- Wentworth, C.K., 1922. A scale of grade and class terms for clastic sediments. *J. Geol.* 30, 377–392.
- Whitman, W.C., Siggeirsson, E.I., 1954. Comparison of line interception and point contact methods in the analysis of mixed grass range vegetation. *Ecology* 35, 431–436.
- Whitney, B.S., Mayle, F.E., Punyasena, S.W., Fitzpatrick, K.A., Burn, M.J., Guillen, R., Chavez, E., Mann, D., Pennington, R.T., Metcalfe, S.E., 2011. A 45 kyr palaeoclimate record from the lowland interior of tropical South America. *Palaeogeogr. Palaeoclimatol. Palaeoecol.* 307, 177–192.
- Xu, Q., Tian, F., Bunting, M.J., Li, Y., Ding, W., Cao, X., He, Z., 2012. Pollen source areas of lakes with inflowing rivers: modern pollen influx data from Lake Baiyangdian, China. *Quat. Sci. Rev.* 37, 81–91.
- Zocatelli, R.O., Amorim, M.A., Cecanho, F., Bernardes, M.C., Moreira-Turcq, P., Turcq, B., Sifeddine, A., Cordeiro, R.C., 2011. Uso dos fenóis da lignina no estudo da matéria orgânica na Várzea do Lago Grande de Curuá, Pará e na Lagoa do Caçó, Maranhão, Brasil. *Acta Amazon.* 41, 195–204.